ISSN 0036-0236, Russian Journal of Inorganic Chemistry, 2007, Vol. 52, No. 5, pp. 753–760. © Pleiades Publishing, Inc., 2007.
Original Russian Text © D.M. Babanly, Yu.A. Yusibov, M.B. Babanly, 2007, published in Zhurnal Neorganicheskoi Khimii, 2007, Vol. 52, No. 5, pp. 819–826.

# Phase Equilibria and Thermodynamic Properties of the System Tl–TlCl–Se

**D. M. Babanly, Yu. A. Yusibov, and M. B. Babanly**
*Rasul-zade State University, Khalilov av. 23, Baku, 370148 Azerbaijan*

Received January 28, 2006

**Abstract**—Phase equilibria in the system Tl–Se–Cl were studied in the region Tl–TlCl–Se by DTA, X-ray powder diffraction, emf measurements concentration circuits (–) Tl/glycerol + KCl + TlCl/(Tl–Se–Ce) (+), and microhardness measurements. Several vertical sections, an isothermal section at 400 K, and the liquidus-surface projection were constructed. The primary crystallization regions and homogeneity regions of phases were determined, including the α phase of variable composition based on $Tl_5Se_2Cl$, the only ternary compound of the system. The types and coordinates of invariant and monovariant equilibria on the *T*–*x*–*y* diagram were determined. From the results of emf measurements, the standard thermodynamic functions of formation and the standard entropy were calculated for the compound $Tl_5Se_2Cl$.

**DOI:** 10.1134/S0036023607050166

Previously, the ternary system Tl–Se–Cl was studied only along the quasi-binary sections $TlCl–Tl_2Se$ [1] and TlCl–TlSe [2]. According to work [1], the system $TlCl–Tl_2Se$ forms a single ternary compound, $Tl_5Se_2Cl$, which melts incongruently by a syntectic reaction at 725 K. At the syntectic temperature, the immiscibility region extends from 15 to 80 mol % $Tl_2Se$. The compound $Tl_5Se_2Cl$ forms a eutectic with TlCl (5 mol % $Tl_2Se$, 689 K) and a peritectic with $Tl_2Se$ (~93 mol % $Tl_2Se$, 684 K). The peritectic reaction $L + Tl_5Se_2Cl \rightleftharpoons \alpha$ produces the $Tl_2Se$-base solid solution, which extends to 18 mol % TlCl [1].

It was determined in work [2] that the system TlCl–TlSe has a simple eutectic phase diagram with the eutectic degenerate at TlSe.

The compound $Tl_5Se_2Cl$ crystallizes in a $Cr_5B_3$-type tetragonal structure with the following unit cell parameters: $a = 8.565$ Å, $c = 12.741$ Å, $Z = 4$, space group *P*4/*ncc* [3]. The lower thallium selenide $Tl_5Se_{3-x}$ ($0.06 < x < 0.5$) has the same structure [4]. Thallium telluride $Tl_5Te_3$ [5, 6] and other compounds of the general formula $Tl_5X_2Hal$ (where X = Se, Te; Hal = Cl, Br, I), which also crystallize in the $Cr_5B_3$-type structure, have higher symmetry (space group *I*4/*mcm*) [1, 3, 7–9]. Thus, the $Tl_5X_2Hal$ compounds are ternary structural analogues of $Tl_5Se_{3-x}$ and $Tl_5Te_3$; they are produced by the substitution of anions $Hal^-$ for anions $X^{2-}$. Ternary analogues of $Tl_5Se_{3-x}$ and $Tl_5Te_3$ obtained by cation substitutions are also known: $Tl_4B^{IV}X_3$ and $Tl_4B^{V}X_6$ ($B^{IV}$ = Sn, Pb; $B^{V}$ = Sb, Bi; X = Se, Te) [10–17].

Analysis of phase diagrams for the systems Tl–X [18–20] and $Tl–B^{IV}(B^{V})–X$ [10–15] shows that both $Tl_5Se_{3-x}$ and $Tl_5Te_3$ and their ternary analogues are phases of variable composition; the homogeneity regions of the ternary compounds extend far beyond the quasi-binary joins $Tl_2X–B^{IV}X$ and $Tl_2X–B_2^{V}X_3$, forming extensive fields along the isothermal sections of *T*–*x*–*y* diagrams. The same situation was observed in the systems Tl–TlI–Se [7] and Tl–TlI–Te [8]. This proves the pertinence of the investigation of phase equilibria over wide ranges of compositions in other Tl–X–Hal systems. Such data are also necessary for the thermodynamic investigation of ternary systems by the emf method [14, 15, 20].

In view of the above, we studied the system Tl–Se–Cl over a wide range of compositions. The results of the restudy of the quasi-binary section TlCl–TlSe described in work [21] differ qualitatively from the data in above-cited work [2]. According to work [21], this section has eutectic equilibrium (85 mol % TlSe, 593 K) and monotectic equilibrium (685 K). At the monotectic temperature, the immiscibility region extends from 15 to 70 mol % TlSe.

The sections $Tl_5Se_2Cl$–TlSe and $Tl_5Se_2Cl$–Tl [22] are non-quasi-binary by virtue of the syntectic melting character of $Tl_5Se_2Cl$, but they are stable below the solidus. An extensive $Tl_5Se_2Cl$-base homogeneity region was found along the section $Tl_5Se_2Cl$–TlSe and an extensive three-phase immiscibility region was found along the section $Tl_5Se_2Cl$–Tl [22].

Here, we report the results of our complex investigation of phase equilibria and thermodynamic properties of the system Tl–Se–Cl in the region Tl–TlCl–Se.

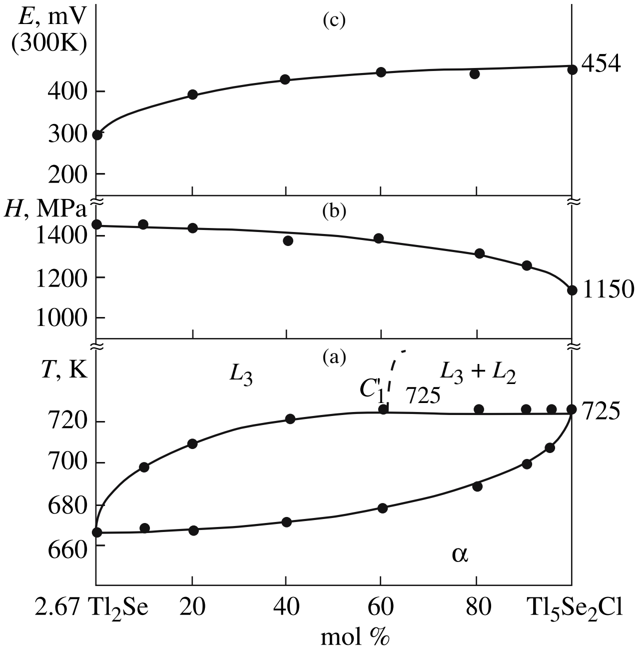

**Fig. 1.** (a) $T$–$x$, (b) $H_\mu$–$x$, and (c) $E$–$x$ diagrams for the system $Tl_2Se$–$Tl_5Se_2Cl$.

## EXPERIMENTAL

First, the compounds TlCl, $Tl_2Se$, TlSe and $Tl_5Se_2Cl$ were prepared. $Tl_2Se$ and TlSe were synthesized by the ampoule technique from the high-purity constituent elements ($10^{-3}$ wt % impurities) under vacuum (~$10^{-2}$ Pa). The alloying temperature was 750 K.

Thallium monochloride was prepared as described in work [23]. First, metallic thallium was dissolved at ~350 K in dilute (~7–10 M) sulfuric acid to obtain a $Tl_2SO_4$ solution. Then, to the boiling 2% $Tl_2SO_4$ solution, dilute HCl was added until reaching complete precipitation. After cooling the mother solution, TlCl was separated, washed with ice-cold distilled water, and dried for a long period in a drier at 390–400 K.

Alloying the thus prepared TlCl with elementary thallium and selenium in required proportions in a evacuated silica ampoule, we obtained the ternary compound $Tl_5Se_2Cl$. In view of the syntectic melting character of this compound, the sample after alloying was heat-treated at 710 K for 100 h.

All compounds synthesized were identified by DTA and X-ray powder diffraction.

Alloying the precursor compounds with elementary selenium and thallium in various proportions in evacuated silica ampoules, we prepared alloys of the system Tl–TlCl–Se with compositions lying along the sections TlCl–$Tl_2Se$, TlCl–Se, $Tl_2Se$–[$Tl_2Cl$] (hereafter, heterogeneous alloys taken as a “component” are indicated in parentheses), $Tl_2Se$–[TlSeCl], and $Tl_5Se_2Cl$–Se, as well as several samples outside these sections. The sample size in DTA experiments was 0.5 g; in the other experiments, it was 1 g.

From the results of the DTA of cast unhomogenized samples, the annealing temperatures were chosen at which these samples were exposed for periods of 500 to 1000 h. Particular attention was paid to the equilibration of the alloys with compositions lying along the section TlCl–$Tl_2Se$ and in the region $Tl_5Se_2Cl$–$Tl_2Se$–$Tl_5Se_{2.94}$ (the boundary composition of the phase $Tl_5Se_{3-x}$). After alloying at 770–780 K, the samples were stepwise annealed. First, they were exposed at 690 K for 500 h; then, they were slowly (for 10 h) cooled to 650 K and exposed for another 500 h.

The investigative tools were DTA (pyrometer NTR-75, chromel–alumel thermocouples), X-ray powder diffraction (diffractometer DRON-2, Cu$K_\alpha$ radiation), microhardness measurements (tester PMT-3), and emf measurements in the concentration circuits

$$(-)\ \text{Tl(solid)/liquid electrolyte} + \text{Tl}^+\text{/(Tl–Se–Cl)(solid)}(+) \qquad (1)$$

from 300 to 430 K. The electrolyte was a glycerol solution of KCl with ~0.1 wt % TlCl. The left-hand electrode was metallic thallium. The right-hand electrodes were presynthesized equilibrium alloys from the region TlCl–$Tl_2Se$–Se of the system Tl–TlCl–Se.

The emf was measured by a compensation technique using a high-resistance digital voltmeter V-7-34A. The composition of circuits (1) and the emf measurement procedure were the same as in works [14, 15, 20].

## RESULTS AND DISCUSSION

The investigation of carefully annealed alloys along the previously studied section TlCl–$Tl_2Se$ showed that our results (Fig. 1) in the region TlCl– $Tl_5Se_2Cl$ coincide with the data in work [1] but are slightly different in the region $Tl_5Se_2Cl$–$Tl_2Se$.

The system $Tl_2Se$–$Tl_5Se_2Cl$ (Fig. 1a) forms complete solid solutions: the solidus temperature increases continuously from 663 K in $Tl_2Se$ to 725 K in $Tl_5Se_2Cl$. The horizontal at 725 K proves the existence of immiscibility in the region ~40–100 mol % $Tl_5Se_2Cl$, which matches the data in work [1]. However, we have not confirm the existence of the peritectic horizontal at 684 K indicated in work [1] (Fig. 1a).

The powder X-ray diffraction, microhardness (Fig. 1b), and emf (Fig. 1c) data confirm the DTA data. From Figs. 1b and 1c, one can see that the microhardness and emf in the $Tl_2Se$–$Tl_5Se_2Cl$ alloys are continuous functions of composition: their value vary monotonically between the $H$ and $E$ of the starting compounds. The single-phase constitution of each sample is proven by the fact that a single microhardness value was measured. The continuous variation in the emf of circuit (1) over a wide range from 280 mV in $Tl_2Se$ to 454 mV in

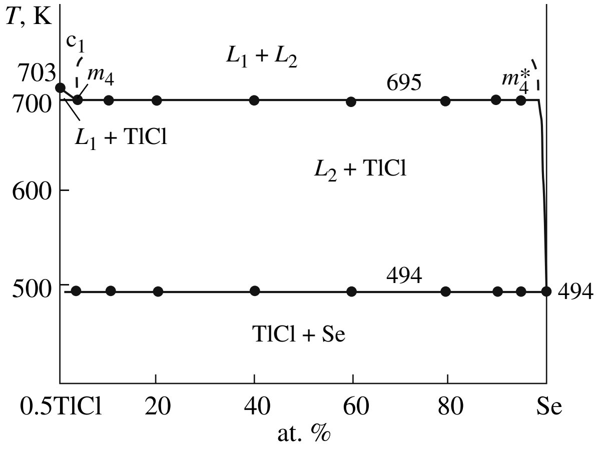

**Fig. 2.** TlCl–Se phase diagram.

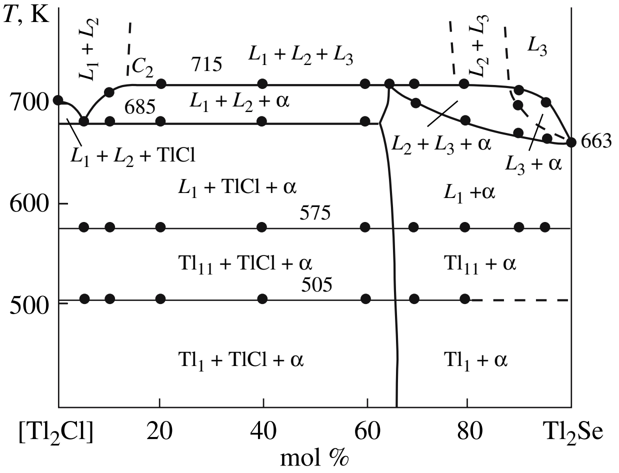

**Fig. 3.** Vertical section $[Tl_2Cl]$–$Tl_2Se$ of the Tl–TlCl–Se phase diagram.

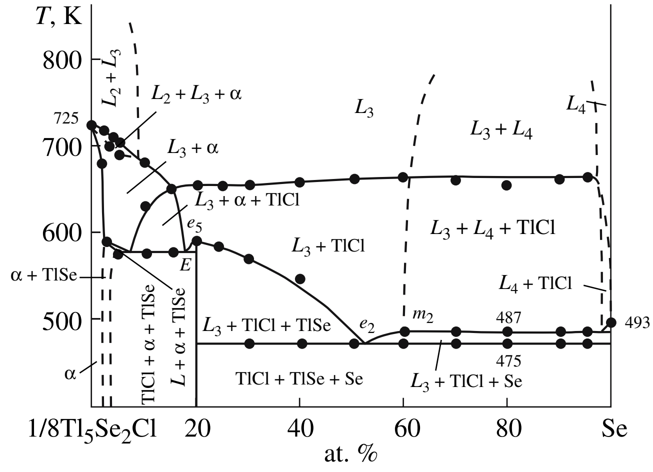

**Fig. 4.** Vertical section $Tl_5Se_2Cl$–Se of the Tl–TlCl–Se phase diagram.

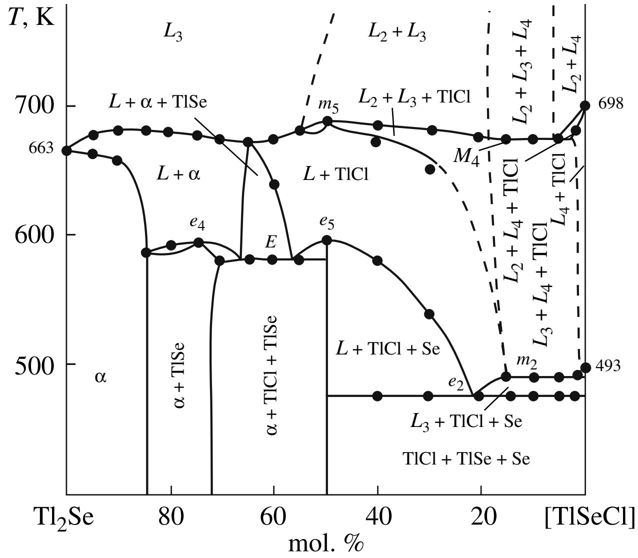

**Fig. 5.** Vertical section $Tl_2Se$–[TlSeCl] of the Tl–TlCl–Se phase diagram.

$Tl_5Se_2Cl$ indicates [20] the continuous variation in the activity of the potential-forming element (thallium) in the alloys, which provides circumstantial evidence of the change in the composition of the α phase.

Analysis of the powder X-ray diffraction patterns of annealed $Tl_2Se$–$Tl_5Se_2Cl$ alloys showed that all samples (20, 40, 60, and 80 mol % $Tl_5Se_2Cl$) are a single phase and have a $Tl_2Se$-type tetragonal structure. The unit cell parameters of the α phase vary almost linearly from $Tl_2Se$ to $Tl_5Se_2Cl$ ($a$ = 8.522–8.561 Å; $c$ = 12.68–12.74 Å).

From the DTA data for all the alloys studied with account for the data available on the vertical sections TlCl–$Tl_5Se_2Cl$ [1], TlCl–TlSe [21], and $Tl_5Se_2Cl$–TlSe(Tl) [22] and on the subsystem Tl–Se [18], we derived the complete and self-consistent pattern of phase equilibria in the system Tl–TlCl–Se (Figs. 2–7; Tables 1, 2).

The section TlCl–Se (Fig. 2) is quasi-binary. Its characteristic features are the virtually complete immiscibility of the components in the liquid state and a degenerate eutectic.

The non-quasi-binary section $[Tl_2Cl]$–$Tl_2Se$ (Fig. 3) reflects the character of phase equilibria in the region Tl–TlCl–$Tl_2Se$ (Figs. 6, 7). Below the solidus, this section crosses the heterogeneous regions Tl + TlCl + α and Tl + α. DTA traces for alloys of this section have up to four peaks. The horizontals at 505 and 575 K are, respectively, due to the polymorphic transition and melting of metallic thallium. The peaks at 715 and

685 K reflect four-phase syntectic equilibrium $C_2$ and monotectic equilibrium $M_1$ (Fig. 7, Table 1). The section $[Tl_2Cl]$–$Tl_2Se$ in the liquid state crosses four phase fields: an extensive three-phase field $L_1 + L_2 + L_3$ (~15–78 mol % $Tl_2Se$) bounds two two-phase fields, namely, $L_1 + L_2$ (0–15 mol % $Tl_2Se$) and $L_2 + L_3$ (~78–88 mol % $Tl_2Se$); $Tl_2Se$-rich melts are a single phase ($L_3$).

The sections $Tl_5Se_2Cl$–Se (Fig. 4) and $Tl_2Se$–[TlSeCl] (Fig. 5) reflect the character of phase equilibria in the region TlCl–$Tl_2Se$–Se. Both sections in their subsolidus region cross all four phase fields (α, α + TlSe, α + TlCl + TlSe, and TlCl + TlSe + Se). They fully match the $T$–$x$–$y$ diagram (Figs. 6, 7; Tables 1, 2) and allow us to refine the primary crystallization regions and the coordinates of invariant points of the system Tl–TlCl–.

The isothermal section at 400°C of the Tl–TlCl–Se phase diagram (Fig. 6) consists of six phase fields. The homogeneity region of the α phase extends significantly (to 4 mol %) into selenium-rich compositions outside the quasi-binary system $Tl_2Se$–$Tl_5Se_2Cl$. This is clearly demonstrated by the vertical sections $0.25Tl_5Se_2Cl$–TlSe [22] and $Tl_2Se$–[TlSeCl] (Fig. 5): the homogeneity region of the α phase extends from 0 to 13 mol % TlSe and from 100 to 85 mol % $Tl_2Se$, respectively. The existence of the extensive region of α solid solution generates the two-phase regions α + $Tl_1$ and α + TlSe (Fig. 6). In the three-phase regions α + $Tl_1$ + TlCl, α + TlCl + TlSe, and TlCl + TlSe + Se, the compositions of all coexisting phases, except for the α phase, virtually coincide with the pure components; that is, the solubility in elementary thallium and selenium and in the compounds TlCl and TlSe is insignificant.

The liquidus surface of the system Tl–TlCl–Se (Fig. 7) consists of three fields, which are generated by the primary crystallization of TlCl, the α phase, and TlSe. The fields of elementary selenium and thallium are degenerate. The characteristic feature of this system is the existence of extensive immiscibility regions with the participation of four liquid phases, namely, metallic thallium ($L_1$), TlCl ($L_2$), the α phase ($L_3$), and elementary selenium ($L_4$), in various combinations. The immiscibility regions occupy to ~90% of the area of the Tl–TlCl–S triangle. There are two extensive three-phase liquid immiscibility regions: $L_1 + L_2 + L_3$ ($C_2C_2^{\mathrm{I}}C_2^*$) and $L_1 + L_2 + L_3$ ($M_TM_T^{\mathrm{I}}M_T^*$), which are surrounded by two-phase liquid immiscibility regions. Hereafter, asterisks mark degenerate points. The first three-phase immiscibility region is generated by the three extensive immiscibility regions existing along the sides of the subsystem Tl–TlCl–$Tl_2Se$ ($m_1m_1^*$, $m_3m_3^*$, and $C_1C_1^{\mathrm{I}}$). The second three-phase immiscibility region is generated by the interaction of two-phase regions $m_2m_2^*$, $m_4m_4^*$, and $m_5m_5^{\mathrm{I}}$, which originate from the boundary systems of the subordinate triangle TlCl–TlSe–Se. Between these three-phase immiscibility regions, there is the extensive two-phase region $L_2 + L_3$.

The crystallization of phases in the indicated immiscibility regions leads to various invariant and monovariant syntectic and monotectic equilibria (Tables 1, 2).

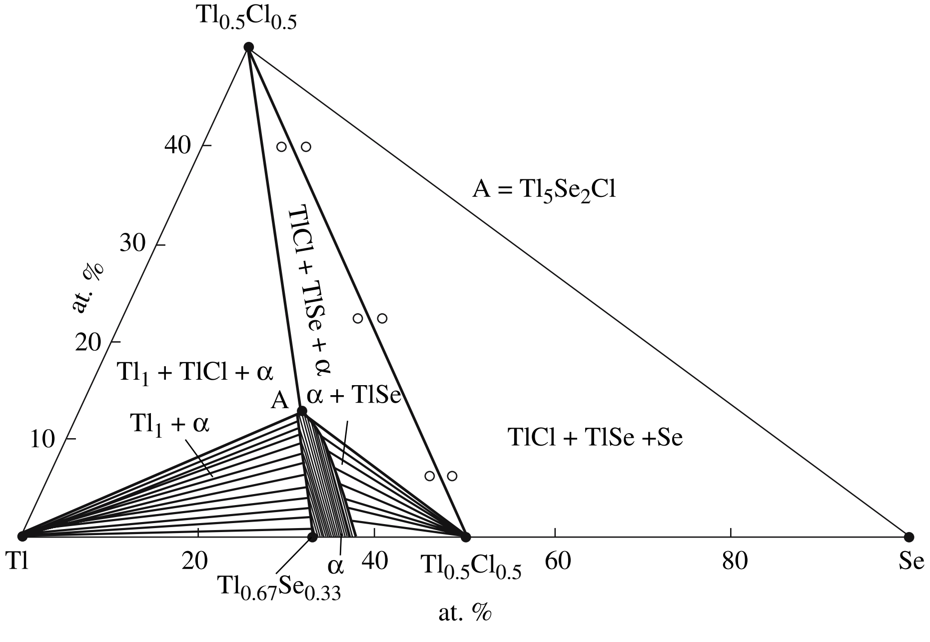

**Fig. 6.** Isothermal section at 400 K of the Tl–TlCl–Se phase diagram. Circles indicate the compositions of the alloys studied by the emf method.

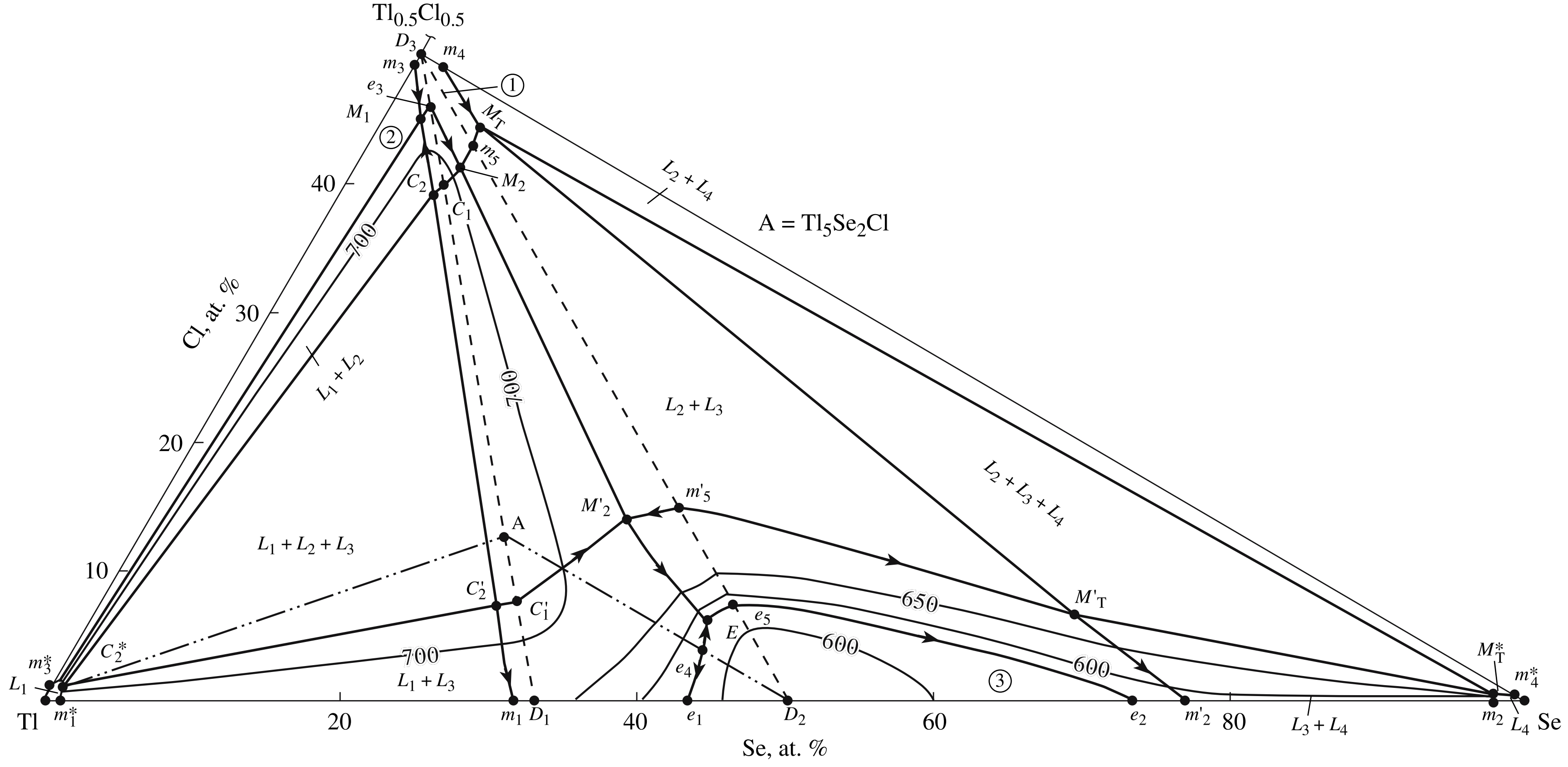

**Fig. 7.** Liquidus surface projection for the system Tl–TlCl–Se. Primary crystallization fields: (*1*) TlCl, (*2*) δ phase with the $Tl_5Se_{3-x}$-type structure, and (*3*) TlSe. Quasi-binary joins stable below the solidus are indicated by dashed lines.

**Table 1.** Invariant equilibria of the system Tl–TlCl–Se

| Point in Fig. 7 | Equilibrium | Composition, at. % | | $T$, K |
|---|---|---|---|---|
| | | Cl | Se | |
| $D_1$ | $\mathrm{L}_{D_1} \rightleftarrows \mathrm{Tl_2Se}$ | – | 33.3 | 663 |
| $D_2$ | $\mathrm{L}_{D_2} \rightleftarrows \mathrm{TlSe}$ | – | 50 | 617 |
| $D_3$ | $\mathrm{L}_{D_3} \rightleftarrows \mathrm{TlCl}$ | 50 | – | 703 |
| $e_1$ | $\mathrm{L} \rightleftarrows \mathrm{Tl_2Se}(\alpha) + \mathrm{TlSe}$ | – | 43 | 580 |
| $e_2$ | $\mathrm{L} \rightleftarrows \mathrm{TlSe} + \mathrm{Se}$ | – | 73 | 475 |
| $e_3$ | $\mathrm{L} \rightleftarrows \mathrm{TlCl} + \mathrm{Tl_5Se_2Cl}(\alpha)$ | 46 | 2.5 | 690 |
| $e_4$ | $\mathrm{L} \rightleftarrows \mathrm{Tl_5Se_2Cl}(\alpha) + \mathrm{TlSe}$ | 3.5 | 42.5 | 590 |
| $e_5$ | $\mathrm{L} \rightleftarrows \mathrm{TlCl} + \mathrm{TlSe}$ | 7 | 43 | 593 |
| $E$ | $\mathrm{L} \rightleftarrows \alpha + \mathrm{TlCl} + \mathrm{TlSe}$ | 6 | 42 | 580 |
| $m_1(m_1^*)$ | $\mathrm{L_3} \rightleftarrows \mathrm{L_1} + \mathrm{Tl_2Se}(\alpha)$ | – | 32.5 | 653 |
| $m_2(m_2^{'})$ | $\mathrm{L_4} \rightleftarrows \mathrm{L_3} + \mathrm{Se}$ | – | 97.5 (77) | 487 |
| $m_3(m_3^*)$ | $\mathrm{L_2} \rightleftarrows \mathrm{L_1} + \mathrm{TlCl}$ | 49 | – | 700 |
| $m_4(m_4^*)$ | $\mathrm{L_2} \rightleftarrows \mathrm{L_4} + \mathrm{TlCl}$ | 48.5 | 3 | 698 |
| $m_5(m_5^{'})$ | $\mathrm{L_2} \rightleftarrows \mathrm{L_3} + \mathrm{TlCl}$ | 42.5 (15) | 7.5 (35) | 685 |
| $C_1(C_1^{'})$ | $\mathrm{L_2} + \mathrm{L_3} \rightleftarrows \mathrm{Tl_5Se_2Cl}(\alpha)$ | 40 (7.5) | 7(28) | 725 |
| $C_2(C_2^{'}\ C_2^*)$ | $\mathrm{L_2} + \mathrm{L_3} \rightleftarrows \mathrm{L_1} + \alpha$ | 38 (7) | 6 (26) | 715 |
| $M_1(M_1^*)$ | $\mathrm{L_2} \rightleftarrows \mathrm{L_1} + \mathrm{TlCl} + \alpha$ | 45 | 2.5 | 685 |
| $M_2(M_2^{'})$ | $\mathrm{L_2} \rightleftarrows \mathrm{L_3} + \alpha + \mathrm{TlSe}$ | 41 (14) | 7.5 (32) | 680 |
| $M_\mathrm{T}(M_\mathrm{T}^{'}, M_T^*)$ | $\mathrm{L_2} \rightleftarrows \mathrm{L_3} + \mathrm{L_4} + \mathrm{TlCl}$ | 44.5 (6.5) | 7 (65) | 673 |

Notes: Conjugate invariant points and their compositions are in parentheses. Asterisks mark virtually degenerate points.

For example, the intersection of the immiscibility regions by the eutectic curves that radiate from point $e_3$ generates in Fig. 7 the horizontals $M_1M_1^*$ and $M_2M_2^{\mathrm{I}}$, which are characterized by four-phase monotectic equilibria.

The types of invariant equilibria and the coordinates of relevant points are listed in Table 1. The types and temperature ranges of monovariant equilibria are displayed in Table 2.

The results of the emf measurements in circuits (1) in the region TlCl–$\mathrm{Tl_2Se}$–Se are in full match with the solid phase diagram and allow us to calculate the thermodynamic functions for $\mathrm{Tl_5Se_2Cl}$. Recall that the emf is a monotone function of composition within the homogeneity region of the α phase (Fig. 1c). We also determined that within either of the three-phase regions α + TlCl + TlSe and TlCl + TlSe + Se, the emf is unaffected by the bulk composition of the alloys. In the region TlCl + TlSe + Se, the numerical emf values coincide accurate to ±3 mV with the data for pure TlSe [24]. First, this proves the reversibility of circuits (1) [20] and second, supports the insignificant TlSe-base solubility we found in the system Tl–TlCl–Se.

The thermodynamic functions for $\mathrm{Tl_5Se_2Cl}$ were calculated from the emf measurements of circuits (1) in the three-phase region α($\mathrm{Tl_5Se_2Cl}$)–TlCl–TlSe using the procedure described in work [20]. The least-squares fits [25] in accordance with the recommendation in work [26] yielded the linear equation for the emf versus temperature in the specified three-phase field:

$$E,\ \mathrm{mV} = 473.3 - 0.066T$$

$$\pm 2[(1.57/22) + 5.1\times10^{-5}(T - 362.8)^2]^{1/2}.$$

Using known thermodynamic relationships, from this equation we calculated the relative partial molar functions for thallium in the region at 298 K:

$$\Delta\bar{G}_{\mathrm{Tl}} = -(43.77 \pm 0.10)\ \mathrm{kJ/mol};$$

$$\Delta\bar{H}_{\mathrm{Tl}} = -(45.67 \pm 0.05)\ \mathrm{kJ/mol};$$

$$\Delta\bar{S}_{\mathrm{Tl}} = -(6.37 \pm 1.38)\ \mathrm{J/(mol\ K)}.$$

**Table 2.** Monovariant equilibria of the system Tl–TlCl–Se

| Curve in Fig. 7 | Equilibrium | Temperature range, K |
|---|---|---|
| $e_3M_1$ | $L \rightleftarrows TlCl + Tl_5Se_2Cl(\alpha)$ | 690–685 |
| $e_3M_2$ | $L \rightleftarrows TlCl + \alpha$ | 690–680 |
| $e_4e_1$ | $L \rightleftarrows \alpha + TlSe$ | 590–580 |
| $e_4E$ | $L \rightleftarrows \alpha + TlSe$ | 590–580 |
| $e_5E$ | $L \rightleftarrows TlCl + TlSe$ | 593–580 |
| $e_5e_2$ | $L \rightleftarrows TlCl + TlSe$ | 593–475 |
| $C_1C_2\,(C'_1C'_2)$ | $L_2 + L_3 \rightleftarrows Tl_5Se_2Cl(\alpha)$ | 725–715 |
| $C_1M_2\,(C'_1M'_2)$ | $L_2 + L_3 \rightleftarrows Tl_5Se_2Cl(\alpha)$ | 725–680 |
| $C_2M_1$ | $L_2 \rightleftarrows L_1 + Tl_5Se_2Cl(\alpha)$ | 715–685 |
| $C'_2\,m_1$ | $L_2 \rightleftarrows L_1 + \alpha$ | 715–653 |
| $m_3M_1$ | $L_2 \rightleftarrows L_1 + TlCl$ | 700–685 |
| $m_5M_2\,(m'_5M'_2)$ | $L_2 \rightleftarrows L_3 + TlCl$ | 685–680 |
| $m_5M_T(m'_5M'_T)$ | $L_2 \rightleftarrows L_3 + TlCl$ | 685–673 |
| $m_4M_T$ | $L_2 \rightleftarrows L_4 + TlCl$ | 698–673 |
| $M'_T\,m'_2$ | $L_2 \rightleftarrows L_4 + TlCl$ | 673–487 |

Note: Conjugate monotectic curves are in parentheses.

According to Fig. 6, these quantities are the thermodynamic functions of the following potential-forming reaction [20]:

$$Tl_{(solid)} + 0.5TlCl_{(solid))} + TlSe_{(solid))} = 0.5Tl_5Se_2Cl_{(solid))}.$$

In accordance with this equation, the standard thermodynamic functions of formation for $Tl_5Se_2Cl$ were calculated from

$$\Delta Z^0(Tl_5Se_2Cl)$$
$$= 2\Delta\bar{Z}_{Tl} + 2\Delta Z^0(TlSe) + \Delta Z^0(TlCl).$$

Here, $\Delta Z = \Delta G$, $\Delta H$, or $\Delta S$. The standard entropy was calculated from

$$S^0(Tl_5Se_2Cl) = 2\Delta\bar{S}_{Tl} + 2S^0(Tl)$$
$$+ S^0(TlCl) + 2S^0(TlSe).$$

**Table 3.** Standard integral thermodynamic functions for compounds TlCl, TlSe, and $Tl_5Se_2Cl$

| Compound | $-\Delta G^0_{298}$ | $-\Delta H^0_{298}$ | $\Delta S^0_{298}$ | $S^0_{298}$ |
|---|---|---|---|---|
| | kJ/mol | | J/(mol K) | |
| TlCl [27] | 184.97 ±<br>± 0.69 | 208.3 ±<br>± 3.0 | –78.3 ±<br>± 1.2 | 111.46 ±<br>± 0.21 |
| TlSe [24] | 60.12 ±<br>± 0.10 | 60.96 ±<br>± 0.54 | –2.8 ±<br>± 1.4 | 103.4 ±<br>± 1.8 |
| $Tl_5Se_2Cl$ | 392.8 ±<br>± 1.1 | 421.6 ±<br>± 5.1 | –96.6 ±<br>± 6.5 | 433.9 ±<br>± 7.2 |

In so doing, we used our own $\Delta\bar{Z}_{Tl}$ data and borrowed from the literature the standard thermodynamic functions for TlCl [27] and TlSe [26] (Table 3) and the standard entropy of elementary thallium [27].

The results of the calculations are displayed in table 3. The errors were determined by error propagation.

## REFERENCES

1. R. Blachnik and H. A. Dreisbach, J. Alloys Compd. **52** (1), 53 (1984).
2. E. Yu. Peresh, V. B. Lazarev, O. I. Korniichuk, et al., Neorg. Mater. **29** (3), 406 (1993).
3. Th. Doert and R. Asmuth, and P. Böttcher, J. Alloys Compd. **209**, 151 (1994).
4. L. I. Man, V. S. Parmon, R. M. Imanov, and A. S. Avilov, Kristallografiya **25** (5), 1070 (1980).
5. L. I. Man, R. M. Imamov, and Z. G. Pinsker, Kristallografiya **16** (1), 122 (1971).
6. I. Schewe and P. Bottcher, Kristallogr. **188** (2), 287 (1989).
7. R. A. Alieva, I. M. Babanly, D. M. Babanly, and I. I. Aliev, Vestn. Bakinsk. Gos. Univ., Ser. Estestv. Nauk, No. 4, 35 (2004).
8. R. A. Alieva, I. M. Babanly, D. M. Babanly, and I. I. Aliev, Zh. Khim. Problem, No. 4, 83 (2004).9. D. M. Babanly, A. A. Nadzhafova, M. I. Chiragov, and M. B. Babanly, *Zh. Khim. Problem*, No. 2, p. 149 (2005).
10. A. A. Gotuk, M. A. Babanly, and A. A. Kuliev, Izv. Akad. Nauk SSSR, Neorg. Mater., **15** (8), 1356 (1979).
11. Yu. V. Voroshilov, M. I. Gurzan, Z. Z. Kish, and L. V. Lada, Izv. Akad. Nauk SSSR, Neorg. Mater. **24** (9), 1479 (1988).
12. Ya. I. Dzhafarov, M. B. Babanly, and A. A. Kuliev, Zh. Neorg. Khim. **43** (8), 1385 (1998) [Russ. J. Inorg. Chem. **43** (8), 1278 (1998)].

13. M. B. Babanly, B. A. Popovkin, I. S. Zamani, and R. R. Guseinova, Zh. Neorg. Khim. **48** (12), 2091 (2003) [Russ. J. Inorg. Chem. **48** (12), 1932 (2003)].
14. M. B. Babanly, A. Akhmad'yar, and A. A. Kuliev, Zh. Neorg. Khim. **30** (4), 1051 (1985).
15. M. B. Babanly, A. Akhmad'yar, and A. A. Kuliev, Zh. Neorg. Khim. **30** (9), 2356 (1985).
16. S. Bradtmoller and P. Bottcher, Z. Anorg. Allg. Chem. **619**, 1155 (1993).
17. Th. Doert and P. Bottcher, Z. Kristalloqr. **209** (1), 96 (1994).
18. N. Kh. Abrikosov et al., *Semiconducting Chalcogenides and Their Base Alloys* (Nauka, Moscow, 1975) [in Russian].
19. M. M. Asadov, M. B. Babanly, and A. A. Kuliev, Izv. Akad. Nauk SSSR, Neorg. Mater. **13** (8), 1407 (1977).
20. M. B. Babanly, Yu. A. Yusibov, and V. T. Abishov, *Electromotive Forces in the Thermodynamics of Compound Semiconductors* (Baku State Univ., Baku, 1992) [in Russian].
21. D. M. Babanly and Yu. A. Yusibov, Zh. Khim. Problem, No. 1, 44 (2006).
22. D. M. Babanly, Z. G. Dzhafarova, and Yu. A. Yusibov, Vestn. Bakinsk. Gos. Univ., Ser. Estestv. Nauk, No. 1, 52 (2006).
23. *Handbuch der pr@aparativen anorganischen Chemie*, Ed. by G. Brauer (Enke, Stuttgart, 1978; Mir, Moscow, 1985).
24. V. P. Vasil'ev, A. V. Nikol'skaya, and Ya. I. Gerasimov, Zh. Fiz. Khim. **45** (8), 2061 (1971).
25. K. Dreffel, *Statistics in Analytical Chemistry* (Mir, Moscow, 1994) [in Russian].
26. A. N. Kornilov, L. B. Stepina, and V. A. Sokolov, Zh. Fiz. Khim. **46** (11), 2974 (1972).
27. *Thermal Constants of Compounds. Handbook*, Ed. by V. P. Glushko (VINITI, Moscow, 1971), Vol. 5 [in Russian].